Polarization modulation of nanotrenches in GaN (0001)/$(000\bar{1})$ by surface hydrogenation

doi: 10.7567/JJAP.56.111002

Polarization modulation of nanotrenches in GaN (0001)/(000-1) by surface hydrogenation

Tomoe Yayama[1, 2]*, Yanlin Gao[3], Susumu Okada[3]*, and Toyohiro Chikyow[2]

[1]*National Institute of Advanced Industrial Science and Technology (AIST), 1-1-1 Umezono, Tsukuba, Ibaraki 305-8568, Japan*

[2]*International Center for Materials Nanoarchitectonics, National Institute for Materials Science (NIMS), 1-1 Namiki, Tsukuba, Ibaraki 305-0044, Japan*

[3] *Graduate School of Pure and Applied Sciences, University of Tsukuba, Tennodai, Tsukuba, Ibaraki 305-8571, Japan*

E-mail: yayama.tomoe@aist.go.jp, sokada@comas.frsc.tsukuba.ac.jp

Using first-principle total-energy calculations within the framework of density functional theory, we show that nanometer scale trenches excavated in GaN with (0001) and (000-1) surfaces cause a variable electrostatic potential difference of up to a few V, which is tunable by controlling the hydrogen coverage of the surfaces. A positive potential difference of 3.53 V is induced between clean (0001) and (000-1) surfaces in nanotrenches. While a negative potential difference of -5.93 V is induced in nanotrenches with fully hydrogenated surfaces. The value of the potential difference strongly depends on the H coverage of the surfaces. Nanotrenches excavated in GaN with polar surfaces can supply electricity for various nanoscale devices consisting of molecules, clusters, and atoms inserted into the trenches.

Keywords: GaN, Nanotrench, Polar surfaces, Hydrogenation, Electronic structures,

1. Introduction

Wide band gap group III nitride semiconductors, such as GaN and its derivatives, have attracted much attention because of their excellent optical and electrical properties for applications as optical and high frequency electronic devices because of their high carrier mobility and wide direct band gap.[1-5] For example, InGaN based quantum well structures have made it possible to realize high performance light-emitting diodes and laser diodes covering the violet to green wavelength regions.[6] Furthermore, the introduction of high-density two-dimensional electron gas at the interfaces in AlGaN/GaN heterostructures mean that GaN-based electronic devices are promising for use in high electron mobility transistors operating with high voltage and low resistivity.[7] GaN with (0001) or (000-1) polar surfaces intrinsically possesses an internal electric field due to a Wurtzite crystal structure consisting of different chemical species.[8-10] For optical device applications, the spontaneous and piezoelectric polarization of GaN suppresses the device efficacy in some cases, because the polarization of the surfaces modulates the wave function overlap between electrons and holes.[11] Accordingly, it is important to control the electric field of GaN when designing highly efficient optical devices.[12, 13]

Polarization on the surfaces of materials allows us to design functionalities that are applicable over wide technological areas. Polarization can control the geometric and electronic structures of atoms and molecules adsorbed on the surfaces and enhances the chemical reactivity of those adsorbates. If we are to use polar surfaces in such ways, we must control the surface polarization to make it possible to tune the physical properties and functions. Here, using the polar surfaces of GaN, we propose nanometer scale trenches providing an electrostatic potential difference of a few V whose polarization can be tuned by controlling the hydrogen coverage of the surfaces and their concentrations (Fig. 1). Using density functional theory with the generalized gradient approximation, we investigated the electronic structures of nanoscale trenches excavated in GaN with (0001) and (000-1) surfaces. Our calculations show that the nanotrenches cause a variable potential difference of up to a few V, which can be tuned by controlling the hydrogen coverage of the surfaces. The potential difference can induce an electric field of MV/cm order that is comparable to the field derived from piezoelectric polarization in several nm regions. The results mean that the trenches can provide the electricity supply for nanoscale

electronic devices consisting of atoms and molecules sandwiched between the trenches. In this paper, the concept of potential difference control with hydrogenation in the nanotrenches is shown by using ideal and reconstructed surface models.

2. Calculation methods

All calculations were performed based on a density functional theory framework[14,15] using the VASP[16] and STATE[17] packages. To calculate the exchange-correlation potential among interacting electrons, we used the generalized gradient approximation (GGA) with the Perdew-Burke-Ernzerhof (PBE) functional form.[18] For the electron-ion interaction, we used the potential generated by the projector augmented wave (PAW) method and an ultrasoft scheme for the VASP and STATE calculations, respectively. The valence wave functions were expanded in terms of a plane wave basis set with cutoff energies of 800 eV for the PAW potentials and 340 eV for the ultrasoft pseudopotentials. Integration over the Brillouin zone was carried out using a Monkhorst-Pack 7x7x1 k-point mesh. For the STATE package, we use the effective screening medium (ESM) method to simulate the GaN thin films under an open boundary condition normal to the slabs to exclude the unphysical dipole interaction with the image cells arising from the surface polarization.[19] Structural optimization was performed until the remaining force acting on each atom was less than 5 mRy/Å for a lateral lattice constant of 3.249 Å corresponding to a 2x2 cell with GaN (0001)/(000-1) surfaces.

To evaluate the surface stability under the different hydrogen condition, we calculate the formation energy of GaN (0001)/(000-1) surfaces (ΔE_f) as

$$\Delta E_f = E_{\mathrm{tot}} - E_{\mathrm{ref}} - n_{\mathrm{Ga}}\mu_{\mathrm{Ga}} - n_{\mathrm{N}}\mu_{\mathrm{N}} - n_{\mathrm{H}}\mu_{\mathrm{H}} \quad (1)$$

where E_{tot}, E_{ref}, n_i and μ_i are the total energies of reconstructed and ideal (0001)/(000-1) surfaces, the number of excess atoms, and chemical potential of an element i (i = Ga, N, H) in the slab. The μ_{Ga} and μ_{N} satisfy the condition that the surface is in equilibrium with bulk GaN described as

$$\mu_{\mathrm{Ga}} + \mu_{\mathrm{N}} = \mu_{\mathrm{GaN}}^{\mathrm{bulk}} \quad (2)$$

where $\mu_{\mathrm{GaN}}^{\mathrm{bulk}}$ is the chemical potential of bulk GaN. Generally, the following formulas hold: $\mu_{\mathrm{Ga}} \leq \mu_{\mathrm{Ga}}^{\mathrm{bulk}}$, $\mu_{\mathrm{N}} \leq \mu_{\mathrm{N2}}^{\mathrm{molecule}}$, $\mu_{\mathrm{H}} \leq \mu_{\mathrm{H2}}^{\mathrm{molecule}}$. $\mu_{\mathrm{Ga}}^{\mathrm{bulk}}$, $\mu_{\mathrm{N2}}^{\mathrm{molecule}}$, $\mu_{\mathrm{H2}}^{\mathrm{molecule}}$ are the

chemical potential per atom of the elements Ga, N, H in their standard states. Using above inequalities and eq. (2), μ_{Ga}has a value in the range $\mu_{\mathrm{Ga}}^{\mathrm{bulk}} + \Delta H \leq \mu_{\mathrm{Ga}} \leq \mu_{\mathrm{Ga}}^{\mathrm{bulk}}$ i.e. $\Delta H \leq \Delta\mu_{\mathrm{Ga}} \leq 0$ where $\Delta\mu_{\mathrm{Ga}} = \mu_{\mathrm{Ga}} - \mu_{\mathrm{Ga}}^{\mathrm{bulk}}$. Here, ΔH is the heat of formation of GaN and the calculated value in this work is -0.94 eV. In the same manner, $\Delta\mu_{\mathrm{H}} = \mu_{\mathrm{H}} - \mu_{\mathrm{H2}}^{\mathrm{molecule}} \leq 0$ is true. Using Eq. (2), Eq. (1) can be expressed as

$$\Delta E_f = E_{\mathrm{tot}} - E_{\mathrm{ref}} - (n_{\mathrm{Ga}} - n_{\mathrm{N}})\mu_{\mathrm{Ga}}^{\mathrm{bulk}} - n_{\mathrm{N}}\mu_{\mathrm{GaN}}^{\mathrm{bulk}} - n_{\mathrm{H}}\mu_{\mathrm{H2}}^{\mathrm{molecule}} - (n_{\mathrm{Ga}} - n_{\mathrm{N}})\Delta\mu_{\mathrm{Ga}} - n_{\mathrm{H}}\Delta\mu_{\mathrm{H}} \quad (3)$$

where E_{tot}, E_{ref}, $\mu_{\mathrm{Ga}}^{\mathrm{bulk}}$, $\mu_{\mathrm{GaN}}^{\mathrm{bulk}}$, and $\mu_{\mathrm{H2}}^{\mathrm{molecule}}$are calculated by the DFT. Considering the experimental conditions, GaN thin film growth is usually performed N-rich environment. Therefore, we chose the value $\Delta\mu_{\mathrm{Ga}} = \Delta H$ in this work.

3. Results and discussion

Figure 1 shows the plane-averaged electrostatic potential of GaN thin films consisting of 20 atomic layers with clean (Fig. 1 (a)) and hydrogenated surfaces (Fig. 1 (b)) by using the ESM method. In accordance with the use of the ESM method, we can estimate the electrostatic potential of (0001) and (000-1) surfaces of GaN thin films. For the calculations, to simulate an isolated GaN slabs, the cell boundaries are located by about 5 A above and below the top- and the bottom-most atomic sites, respectively. The position of the atoms is indicated in the figure. Open, gray and black filled circles show the Ga, N and H atoms, respectively. The shallow and deep electrostatic potentials correspond to Ga and N, respectively. For a thin film with clean surfaces, the electrostatic potential just above the N surface ((000-1) surface) is higher than that above the Ga ((0001) surface). In contrast, the potential difference between the N and Ga surfaces of the hydrogenated GaN thin film is opposite to that of the thin film with clean surfaces. Thus, surface hydrogenation can tune the polarity of GaN thin films with (0001)/(000-1) surfaces. The inversion of polarity with hydrogenation is induced by positively and negatively charged H atoms attached to the N and Ga atoms, respectively. Pseudoatoms with valence electrons of 0.75e and 1.25e are needed to saturate the valence states of surface N and Ga atoms, respectively.[20] Therefore, the neutral H atoms on the surface induce excess and deficit electrons on the N and Ga surfaces, respectively, resulting in polarity opposite to that of the sheet with clean surfaces. The similar case of polarity control with hydrogenation for

BN nano-ribbon has been reported.[21)]

The polarity control of GaN thin films caused by hydrogenation allows us to design a nanoscale electric power supply whose field direction can be tuned by controlling the hydrogen concentration. Here, we focus on nanometer scale trenches with GaN-(0001) (c plane) and (000-1) (-c plane) polar surfaces. The surfaces of the trenches are simulated with an ideal 2x2 atomic structure, although the surfaces possess various reconstructed structures.[22-26)] The trenches are simulated under periodic boundary condition for a-, b- and c-direction by a repeated slab model of GaN consisting of 20 atomic layers with clean and hydrogenated c and c- surfaces (Fig. 2), which are separated with a 2nm spacing. Owing to the model, the potential gradient or electric field emerges in the 2nm wide. To investigate the polarity in the trenches with respect to the hydrogen concentration, we also consider various hydrogenation patterns on the (0001)/(000-1) surfaces of GaN. In the figure 3, the schematic views of the hydrogenation patterns on the (0001) surfaces are shown. Open, gray and black filled circles show the Ga, N and H atoms, respectively. The large or mid-circle size indicate that the atoms are in the topmost or second layer.

Figure 4 shows the plane-averaged electrostatic potential normal to the trench with various hydrogen concentrations ranging from 0 to 100%. Here, the same coverage is applied to both (0001) and (000-1) surfaces symmetrically: Fig. 4(a) is the result of the ideal surfaces, i.e. 0% coverage; Figs. 4(b)-(e) show the results of 25-100% covered surfaces for both (0001) and (000-1). First, we can see the polarity inverse in clean (0%) and fully hydrogenated (100%) cases. For the clean surfaces, the finite potential gradient arising from the electrochemical difference between the N and Ga atoms is seen between the surfaces of the trench. The calculated potential difference between the surfaces is 3.530 V. When both trench surfaces are fully hydrogenated, the nature of the potential profile is different from that of a trench with clean surfaces. The calculated potential difference is -5.927 V, which is opposite to that in a trench with clean surfaces.

Moreover, the other results indicate that the potential difference in the nanotrench strongly depends on the hydrogen coverage of the surfaces. The positive electrostatic potential difference in the trench was 1.569 V for coverage of 25 %, while the negative voltage was -3.354 V for coverage of 75 %. For 50 % coverage, there was a small positive voltage of 1.111 V. Figure 5 shows the potential difference between the surfaces as a

function of their hydrogen concentration under symmetric hydrogenation. The potential difference decreases monotonically with increasing surface coverage. The neutrality point of the field is located between hydrogen concentrations of 50 and 75 %. This fact indicates that the potential difference between nanotrenches can be controlled by adsorbing/desorbing H atoms to/from the surfaces. At the neutral point, a non-polar condition is realized in GaN nanotrenches with c/-c surfaces, and this is expected to cause unusual phenomena that are not observed with bulk Ga/N surfaces. It should be noted that the local electrostatic potential exhibits a complex profile due to the inhomogeneity of the electron distribution on the surfaces of the nanotrenches.

It is worth investigating the way in which the potential difference between the nanotrenches depends on asymmetric hydrogenation. Table I summarizes the potential difference between nanotrenches in GaN with (0001)/(000-1) surfaces caused by asymmetric hydrogenation. In this case, an inhomogeneous electron density on the surface of a trench induces a complex potential difference depending on the hydrogenation of the (0001) and (000-1) surfaces. For instance, for all hydrogen concentrations on (000-1) surfaces except clear surfaces, the potential difference reaches maximum at a (0001) surface coverage of 50 %. On the other hand, for all hydrogen concentrations on a (0001) surface, the potential difference decreases as the hydrogen concentration increases on a (000-1) surface. This indicates that the delicate balance of electron densities on the surfaces of the nanotrenches leads to an interesting variation in their polarization, which is applicable for controlling the physical properties of foreign materials inserted into the nanotrench by the variable potential difference and electric field.

Since asymmetric hydrogenation on the surfaces affects polarization in the trenches, the potential difference also depends on the mutual arrangement of the hydrogenation on the two surfaces. Figure 6 shows the plane averaged electrostatic potentials for various hydrogenations on the (0001) and (000-1) surfaces of the trench with surface coverage ranging from 25 to 75 %. When the concentration is 25% for both surfaces, the potential difference depends weakly on the relative position of the H atoms attached to the Ga and N atoms [Fig. 6 (a)]. Slightly asymmetric hydrogenation leads to a relatively large potential difference than with symmetric hydrogenation. In contrast, for higher surface H concentrations, the electrostatic potentials in the trenches do not depend on the relative

arrangements of H atoms [Figs. 6 (b) and 6 (c)]. Therefore, this fact indicates that the potential difference induced in the nanotrenches excavated in GaN with (0001) and (000-1) surfaces is tunable by controlling the surface coverage.

Since the surfaces of GaN exhibit various morphologies depending on the environmental conditions, it is worth to discuss the possible surface conformations with respect to the hydrogen chemical potential to give guiding principles to realize the trench structure. Figure 7 shows the formation energy of GaN thin films as a function of the H chemical potential $\Delta\mu_H$ and atomic configurations of (0001) and (000-1) surfaces of GaN slabs. More than several dozens of structures for an orientation and every combination between GaN-(0001) and (000-1) surfaces are evaluated. The reported reconstructed structure[22, 23] such as NH_3+3NH_2, NH_3+3GaH or N_{ad}H+NH_2 for GaN-(0001) surface are also considered. The structure NH_3+3GaH-3H, which correspond to the structures NH_3+3GaH and 3H for (0001) and (000-1) respectively, appears in the window of energy diagram in Fig. 7, which is energetically favorable under H poor condition. Note that the energy of the structure NH_3+3NH_2-3H is out of the range of the figure.

Among representative structures, four structures, ideal-3H, NH_2-3H, N_{ad}H+NH_2-3H and NH_3+3GaH-3H, are thermodynamically favorable. For the (0001) surface, the coverage of the topmost hydrogen decreases with decreasing the chemical potential of H, from NH_3+3GaH-3H (100%), N_{ad}H+NH_2 (50%), NH_2 (25%) to ideal (0%). The structures with 75% coverage are not thermodynamically favorable. On the other hand, for (000-1) surface, the 3H structure is a stable conformation throughout the chemical potential, indicating that the surface coverage is insensitive to the environmental condition because the dangling bonds are fully saturated by hydrogen termination. Thus, four possible combinations of the surface conformations of nanotrenches are expected. The potential difference for these three nanotrenches are -2.994, -1.899, -2.183 and -1.298 V for ideal-3H, NH_2-3H N_{ad}H+NH_2-3H and NH_3+3GaH-3H respectively (Table II). Under the condition, although the polarity inversion does not occur, the potential difference sensitively depends on the surface morphologies of trenches. Therefore, the nanotrench can act as a variable voltage supply by controlling the chemical potential of H which reflects the thermodynamic condition. Remind that further arbitrary potential difference control can be realized by changing the chemical functional group adsorbed on the surfaces.

4. Conclusions

Using first-principle total-energy calculations within the framework of density functional theory, we showed that nanotrenches excavated in GaN with (0001) and (000-1) surfaces caused a variable potential difference of up to a few V, which could be tuned by controlling the hydrogen coverage of the surfaces. A positive potential difference of 2.82 V/nm between the (0001) and (000-1) surfaces was induced in nanotrenches with clean surfaces. In contrast, a potential difference of -5.08 V was induced in nanotrenches with fully hydrogenated surfaces. The value of the potential difference depended strongly on the H coverage of the surfaces. The neutrality point of the voltage was located between 50 and 75 % coverage for symmetric hydrogenation. Although the potential difference depended on the number of H atoms on each surface, the voltage was insensitive to the respective arrangement of the H atoms adsorbed on the two surfaces. Additionally, by changing the surface coverage and the reconstruction according to the chemical potential, it was shown that the potential difference could be changed experimentally. This fact implied that the nanotrenches excavated in GaN with polar surfaces supplied a potential difference and induced an external electric field in nanoscale electronic, mechanical, sensing, and energy devices to control their functions by controlling the electronic and geometric structures of molecules, clusters, and atoms inserted into the trenches.

Acknowledgments

This work was supported by JSPS KAKENHI Grant Numbers JP17H01069, JP16H00898, and JP16H06331 from the Japan Society for the Promotion of Science and the Joint Research Program on Zero-Emission Energy Research, Institute of Advanced Energy, Kyoto University. This work was also supported by LEADER program from Ministry of Education, Culture, Sports, Science and Technology-JAPAN.

References

1) R. J. Molnar, R. Singh, and T. D. Moustakas, Appl. Phys. Lett. **66**, 268 (1995).
2) J. M. Van Hove, R. Hickman, J. J. Klassen, and P. P. Chow, Appl. Phys. Lett. **70** 2282 (1997).
3) Y. Zhao, R. M. Farrell, Y.-R. Wu, and J. S. Speck, Jpn. J. Appl. Phys. **53**, 100206 (2014)
4) D. S. Lee, Z. Liu, and T. Palacios, Jpn. J. Appl. Phys. **53**, 100212 (2014)
5) T. Kachi, Jpn. J. Appl. Phys. **53**, 100210 (2014).
6) H. Zhao, G. Liu, J. Zhang, J. D. Poplawsky, V. Dierolf, and N. Tansu, Opt. Express **19**, A991 (2011).
7) X. Liu, Y. Lu, W. Yu, J. Wu, J. He, D. Tang, Z. Liu, P. Somasuntharam, D. Zhu, W. Liu, P. Cao, S. Han, S. Chen, and L. S. Tan, Sci. Rep. **5**, 14092 (2015).
8) F. Bernardini, V. Fiorentini, and D. Vanderbilt, Phys. Rev. B **57**, R10024 (1998)
9) F. Bernardini and V. Fiorentini, Phys. Rev. B **57**, R9427 (1998)
10) R. Langer, J. Simon, V. Ortiz, N. T. Pelekanos, A. Barski, R. Andre, and M. Godlewski, Appl. Phys. Lett. **74**, 3827 (1999).
11) T. Deguchi, K. Sekiguchi, A. Nakamura, T. Sota, R. Matsuo, S. Chichibu, and S. Nakamura, Jpn. J. Appl. Phys. **38**, L914 (1999).
12) P. Waltereit, O. Brandt, A. Trampert, H. T. Grahn, J. Menniger, M. Ramsteiner, M. Reiche, and K. H. Ploog, Nature **406**, 865 (2000).
13) H. Jeong, S. Y. Jeong, D. J. Park, H. J. Jeong, S. Jeong, J. T. Han, H. J. Jeong, S. Yang, H. Y. Kim, K.-J. Baeg, S. J. Park, Y. H. Ahn, E.-K. Suh, G.-W. Lee, Y. H. Lee, and M. S. Jeong, Sci. Rep. **5**, 7778 (2015).
14) P. Hohenberg and W. Kohn, Phys. Rev. **136**, B864 (1964).
15) W. Kohn and L. J. Sham, Phys. Rev. **140**, A1133 (1965).
16) I. A. Courtney, J. S. Tse, O. Mao, J. Hafner and J. R. Dahn, Phys. Rev. B, **58**, 15583 (1998).
17) Y. Morikawa, K. Iwata, K. Terakura, Appl. Surf. Sci. **169-170**, 11 (2001).
18) J. P. Perdew, K. Burke, and M. Ernzerhof, Phys. Rev. Lett. **77**, 3865 (1996).
19) M. Otani and O. Sugino, Phys. Rev. B **73**, 115407 (2006).
20) K. Shiraishi, J. Phys. Soc. Jpn. **59**, 3455 (1990).

21) A. Yamanaka and S. Okada, Phys. Chem. Chem. Phys., **19**, 9113, (2017).
22) C. G. Van de Walle and J. Neugebauer, Phys. Rev. Lett. **88**, 066103 (2002).
23) C. G. Van de Walle and J. Neugebauer, J. Cryst. Growth **248**, 8 (2003).
24) T. Akiyama, T. Yamashita, K. Nakamura, T. Ito, J. Cryst. Growth **318**, 79 (2011).
25) T. Yayama, Y. Kangawa, and K. Kakimoto, Jpn. J. Appl. Phys. **52**, 08JC02 (2013)
26) Y. Kangawa, T. Ito, A. Koukitu, and K. Kakimoto, Jpn. J. Appl. Phys. **53**, 100202 (2014).

Figure Captions

Fig. 1. (Black and white) Plane averaged electrostatic potential of GaN slab model (a) clean (coverage 0%) and (b) hydrogenated surfaces (coverage 100%) calculated by using ESM method. Large open and small filled circles denote the Ga and N atoms, respectively.

Fig. 2. (Color online) A geometric structure of a hydrogenated nanotrench in GaN with (0001) and (000-1) surfaces. Large, medium, and small circles denote Ga, N, and H atoms, respectively.

Fig. 3. (Black and white) Schematic views of the surface morphologies of hydrogenated GaN-(0001) and (000-1) surfaces for the hydrogen coverage from 0 to 100%. The open, pale shaded, and solid circles denote Ga, N, and H atoms, respectively.

Fig. 4. (Black and white) Plane averaged electrostatic potential of nanotrenches with symmetric hydrogen coverage of (a) 0 (clean surfaces), (b) 25, (c) 50, (d) 75, and (e) 100% (fully hydrogenated surfaces) calculated under periodic boundary conditions. Open and filled circles denote the topmost atoms of (0001) and (000-1) surfaces without and with hydrogen atom, respectively.

Fig. 5. (Black and white) Potential difference in the nanotrenches as a function of hydrogen coverage.

Fig. 6. (Black and white) Plane averaged electrostatic potential of nanotrenches with asymmetric surface coverage of (a) 25, (b) 50, and (c) 75 % hydrogen concentrations calculated under periodic boundary conditions. The values of potential difference are noted together. Open and filled circles denote the topmost atoms of (0001) and (000-1) surfaces without and with hydrogen atom, respectively.

Fig. 7. (Black and white) Surface formation energy depending on the chemical potential of H ($\Delta\mu_{\mathrm{H}}$) and the schematic views of atomic structure of the topmost and the second subsurface atoms of (0001) and (000-1) surfaces for three stable structures. The open, pale shaded, and solid circles denote Ga, N, and H atoms, respectively.

Table I. Potential difference in the nanotrenchs with the hydrogenated GaN-(0001) and (000-1) surfaces for various coverages.

	Potential difference [V]				
	Hydrogen coverage on (0001) plane [%]				
Hydrogen coverage on (000-1) plane [%]	0	25	50	75	100
0	3.530	2.256	2.798	-0.389	-0.651
25	1.169	1.569	1.955	-1.219	-2.147
50	0.471	0.624	1.111	-2.113	-2.814
75	-2.994	-3.007	-2.280	-3.354	-3.869
100	-3.364	-2.874	-2.775	-3.499	-5.927

Table II. Potential difference in the nanotrenchs with the hydrogenated GaN-(0001) and (000-1) surfaces considering the reconstructions. The values for stable three reconstructed structures are listed which are shown in the energy diagram (Fig. 7). There are no data for 75% coverage because these structures are not thermodynamically favorable.

	Potential difference [V]				
	Hydrogen coverage on (0001) plane [%]				
(000-1) plane	0 (ideal)	25 (NH_2)	50 ($N_{ad}H+NH_2$)	75	100 (NH_3+3GaH)
75% (3H)	-2.994	-1.899	-2.183	-	-1.298

Fig.1.

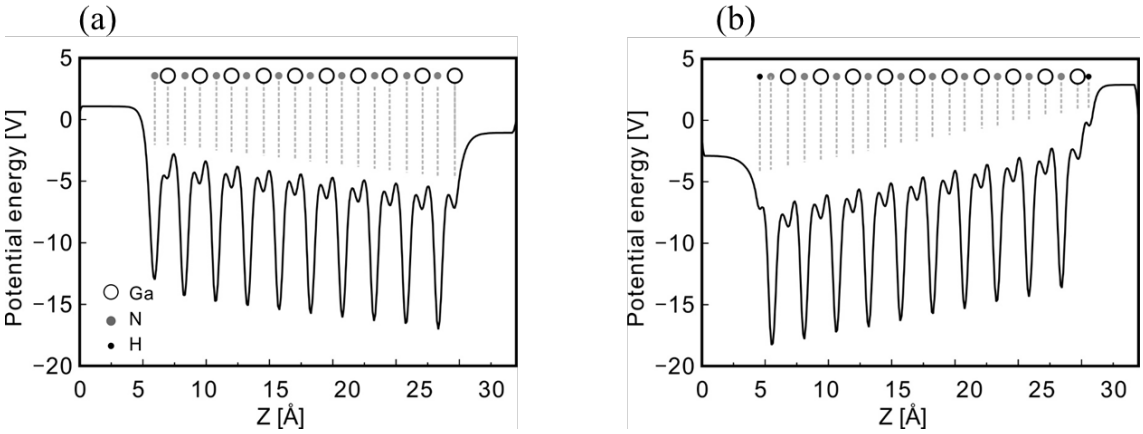

Fig.2 (Color Online)

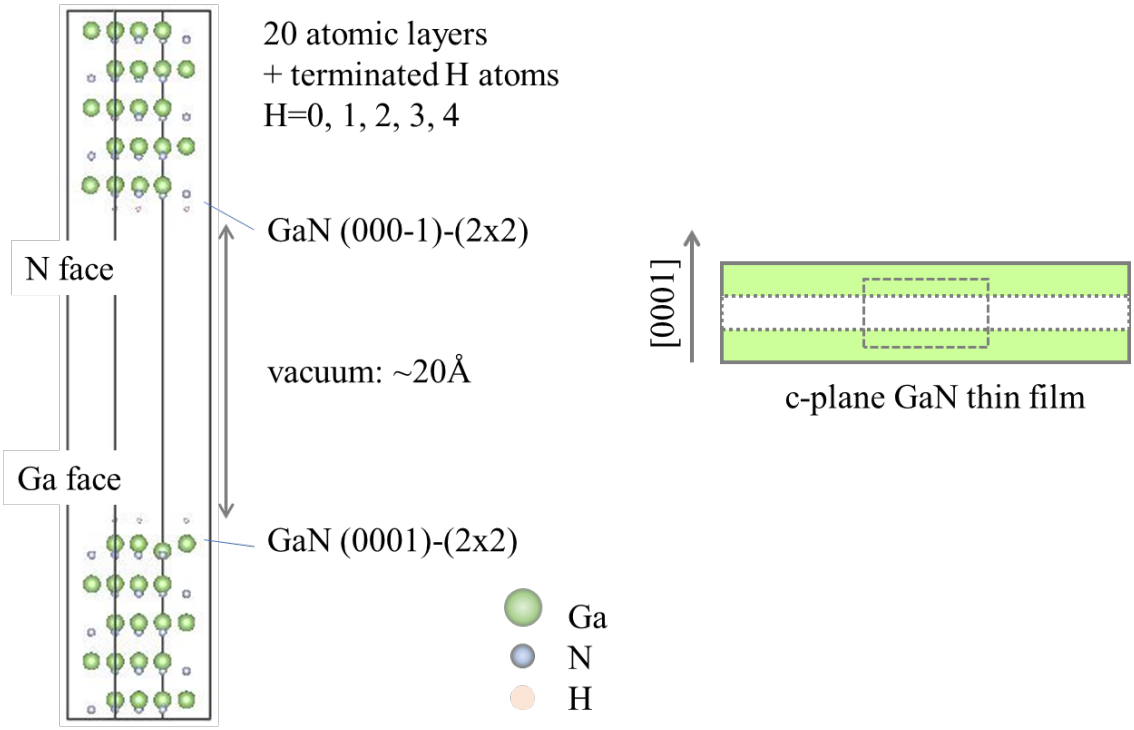

Fig.3

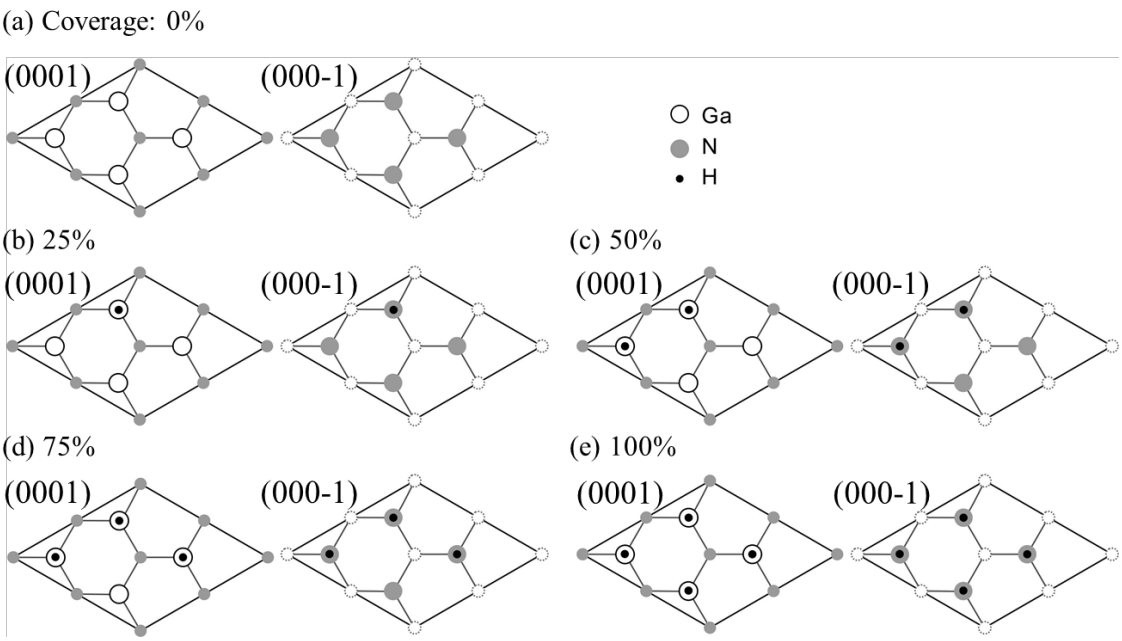
(a) Coverage: 0%
(0001)
(000-1)
Ga
N
H
(b) 25%
(0001)
(000-1)
(c) 50%
(0001)
(000-1)
(d) 75%
(0001)
(000-1)
(e) 100%
(0001)
(000-1)

Fig. 4

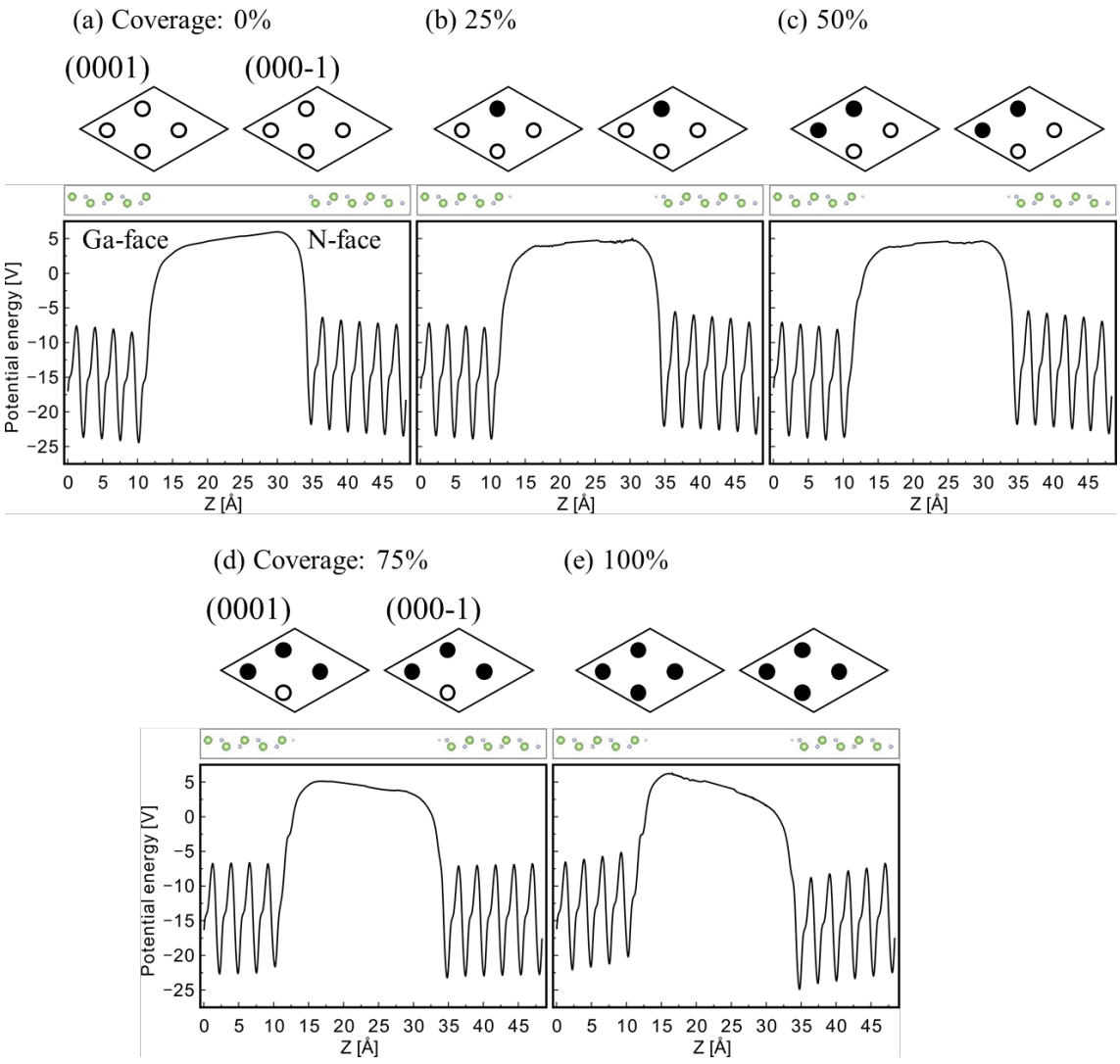
(a) Coverage: 0%
(b) 25%
(c) 50%
(0001)
(000-1)
Ga-face
N-face
Potential energy [V]
Z [Å]
(d) Coverage: 75%
(e) 100%
(0001)
(000-1)
Potential energy [V]
Z [Å]

Fig. 5

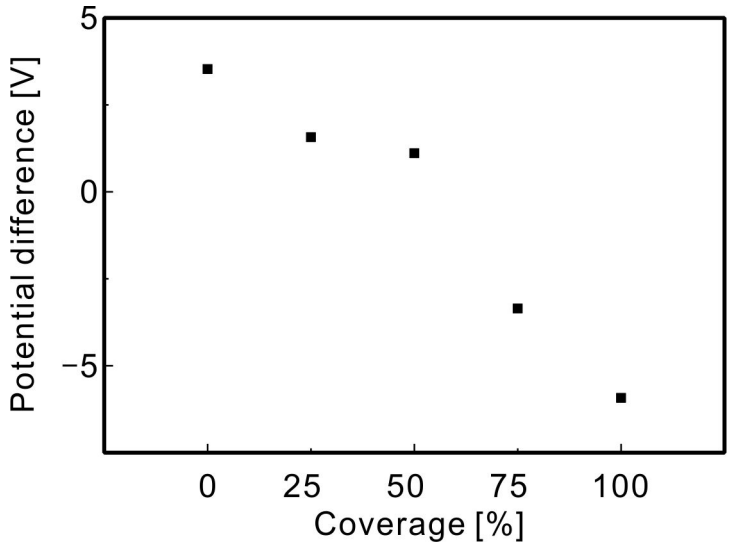
Potential difference [V]
5
0
−5
0
25
50
75
100
Coverage [%]

Fig. 6

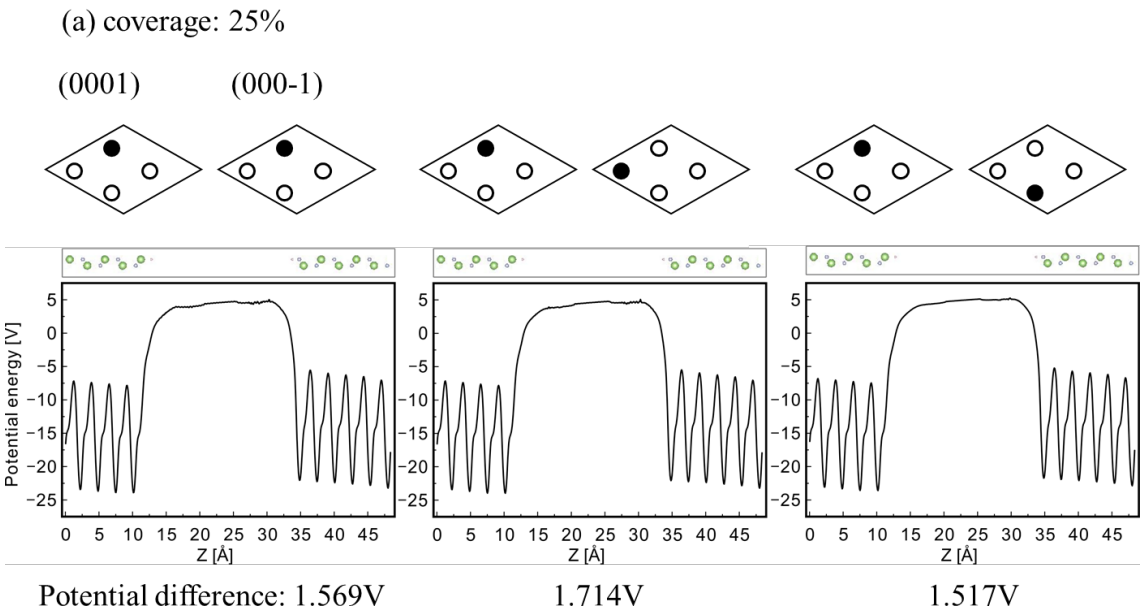
(a) coverage: 25%
(0001)
(000-1)
Potential energy [V]
Z [Å]
Potential difference: 1.569V
1.714V
1.517V

(b) coverage: 50%

(0001) (000-1)

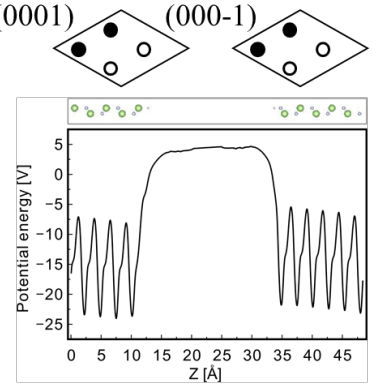

1.111V

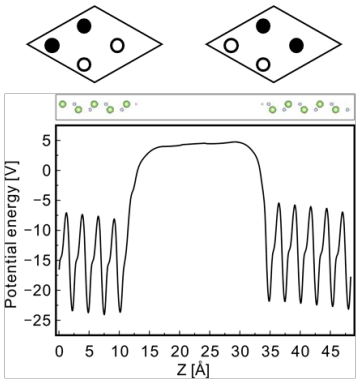

1.218V

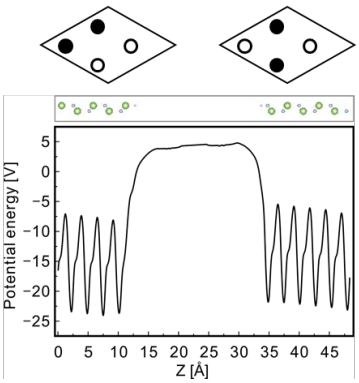

1.158V

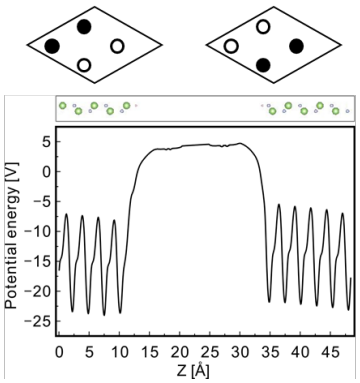

1.106V

(c) coverage: 75%

(0001) (000-1)

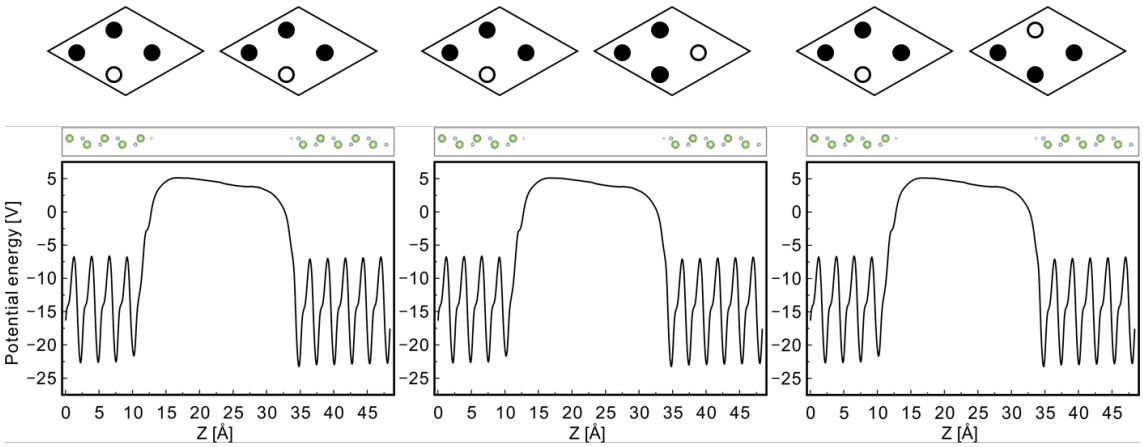

-3.354V -3.327V -3.332V

Fig. 7

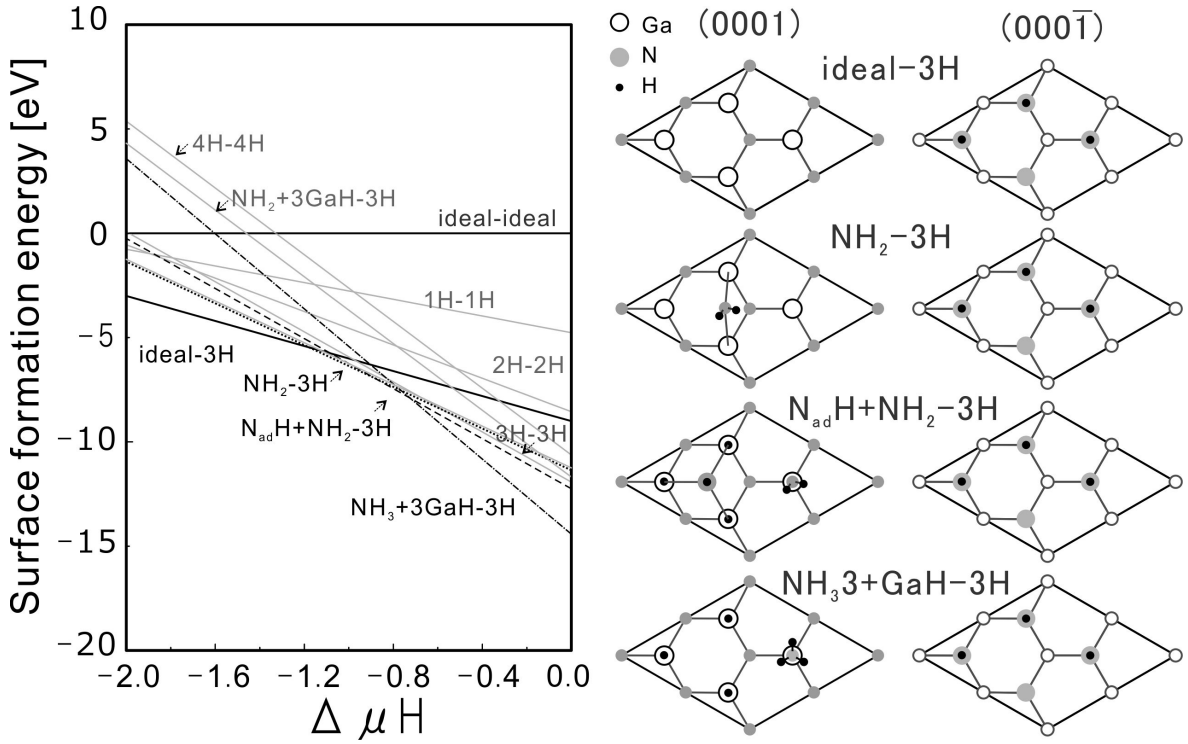
Surface formation energy [eV]
10
5
0
−5
−10
−15
−20
−2.0
−1.6
−1.2
−0.8
−0.4
0.0
Δ μH
4H-4H
NH2+3GaH-3H
ideal-ideal
1H-1H
2H-2H
3H-3H
ideal-3H
NH2-3H
NadH+NH2-3H
NH3+3GaH-3H
Ga
N
H
(0001)
(000$\bar{1}$)
ideal−3H
NH2−3H
NadH+NH2−3H
NH33+GaH−3H